



Denoising ozone concentration measurements with BAMS filtering[☆]

Gabriel Katul^{a,1}, Fabrizio Ruggeri^{b,2}, Brani Vidakovic^{c,*,3}

^aDuke University, Durham, NC 27708-0251, USA

^bCNR - IMATI, I-20133 Milano, Italy

^cGeorgia Institute of Technology, Atlanta, GA 30332, USA

Available online 8 September 2005

Abstract

We propose a method for filtering self-similar geophysical signals infected by an autoregressive noise using a combination of non-decimated wavelet transform and a Bayesian model. In the application part, we consider separating the instrumentation noise from high frequency ozone concentration measurements sampled in the atmospheric boundary layer. The elicitation of priors needed to specify the statistical model in this application is guided by the well-known Kolmogorov **K41**-theory, which describes the statistical structure of turbulent high frequency scalar concentration fluctuations.

© 2005 Elsevier B.V. All rights reserved.

Keywords: Wavelet regression; Shrinkage; Adaptivity; Bayesian models; Ozone

1. Introduction

A variety of geophysical measurements possess inherited self-similarity over a wide range of time scales; for example, turbulent velocities, temperatures and trace gas concentration fluctuations in the atmospheric boundary layer follow the celebrated Kolmogorov's **K41** scaling

[☆] This research was supported, in part, by the National Science Foundation (NSF) Grants DMS-0072585 at Duke University and DMS-0505490 at Georgia Institute of Technology.

* Corresponding author.

E-mail address: brani@bme.gatech.edu (B. Vidakovic).

¹ Gabriel Katul is a Professor at Nicholas School of the Environment and Earth Sciences, Box 90328, Duke University, Durham, NC 27708-0328, USA.

² Fabrizio Ruggeri is a Research Director at Consiglio Nazionale delle Ricerche, Istituto di Matematica Applicata e Tecnologie Informatiche, Via E. Bassini, 15, I-20133 Milano, Italy.

³ Brani Vidakovic is Professor at The Wallace H. Coulter Department of Biomedical Engineering, Georgia Institute of Technology, Atlanta, GA30332, USA.

(Kolmogorov, 1941) for locally homogeneous and isotropic turbulence. Simply stated, the spectrum of such time series exhibits a power-law decay of $-\frac{5}{3}$. This power-law is clearly visible in the wavelet domain when logarithms of averaged level energies are plotted against level numbers. A large body of research connecting wavelets, geophysical time series, and their Fourier spectra now exists; see for example Farge (1992), Farge et al. (1992), Hudgins et al. (1993), Katul and Vidakovic (1998), Kumar and Foufoula-Georgiou (1993, 1994), Vattay and Harnos (1994), Vergassola and Frisch (1991), and Zubair et al. (1991). With increased interest in dry ozone transfer between terrestrial ecosystems and the atmosphere, high frequency ozone gas analyzers are now being developed to specifically resolve such detailed turbulent fluctuations. The signals from these gas analyzers are commonly infected with instrument noise excursions thereby motivating the development of new shrinkage methods.

Statistical modeling in the wavelet domain is now considered an effective shrinkage method because prior information about the time series can be naturally incorporated in the space of associated wavelet coefficients. Prime examples are smoothness, periodicity, and self-similarity properties. According to the Bayesian approach a coherent incorporation of information can be achieved by appropriate selection of model components. For instance, to incorporate information about signal smoothness, variances in the prior on the signal part should decay rapidly to zero. If information about self-similarity is available, then the variances in the prior should decay in a power-law fashion.

The availability of prior information scaling in geophysical measurements is therefore amenable to Bayesian modeling (e.g., Berliner et al., 1999; Wikle et al., 1998; Vidakovic et al., 2000; Shi et al., 2005). Linkage between Bayesian modeling and wavelet shrinkage summarizes aforementioned prior information into a sensible and effective paradigm for signal filtering and estimation. The critical fact is that, under mild conditions, Bayes rules are shrinkers and their application on wavelet coefficients leads to simple and effective estimators of unknown signals; see an example in Vidakovic and Ruggeri (1999).

In the application part, we explore the use of a Bayesian model, calibrated by exact theoretical power laws, to analyze high frequency ozone concentrations measurements contaminated with instrumentation noise at multiple frequencies. The Bayesian model is applied in the wavelet domain with the goal of separating the desired turbulence signal from inherited instrumentation noise. The proposed Bayesian model relies on BAMS (Bayesian Adaptive Multiresolution Shrinker), a technique recently proposed by Vidakovic and Ruggeri (2001). The smooth shrinkage, as opposed to thresholding, is critical in preserving the fractality of the signal. Gas analyzers used in high frequency sampling of ozone concentration tend to convolve the signal with a noise assumed either white or autoregressive. The separation between signal and noise is achieved by inverting wavelet coefficients, split in a fashion dictated by the statistical model which incorporates a **K41** type power-law.

The paper is organized as follows: in Section 2.1, a brief description of the experiment conducted at Duke forest and the time series collected is first presented. Sections 2.2 and 2.3 introduce the statistical model, the BAMS technique, and the specification of model parameters. For completeness, a more detailed description of BAMS rules is given in Appendix A. Batteries of tests, as reported in Section 3, are applied on the split components, both the signal and the noise parts. The signal part is tested against higher order structure functions and mixed moments predicted by **K41** theory while the structure of the noise is analyzed for conformity with the physical properties of the instrument and sampling setup. Concluding remarks, direction of future research, and comparisons with existing methods are further discussed in Section 4.

2. Measurements and model development

We review BAMS, a technique proposed in Vidakovic and Ruggeri (2001) to statistically estimate wavelets coefficients, corresponding to the signal of interest, using a shrinkage rule in a Bayesian framework. The derivation details are reviewed in Appendix A. We start with a brief description of the experimental setup and the measurements collected.

2.1. Experimental setup and data collection

High frequency ozone concentration measurements (O_3) along with air temperature (T) and the three turbulent velocity components (u' , v' , and w') were collected at 40 m from the ground surface over a 33-m tall, 180 year old mixed hardwood forest. These experiments, performed at the Blackwood Division of Duke Forest in Durham, North Carolina, resulted in $60\frac{1}{2}$ -h runs (Katul et al., 1997b). We used such runs, collected over different atmospheric stability conditions, to evaluate the proposed filtering algorithm. The fast-response O_3 gas analyzer employs chemiluminescent reaction of O_3 with eosine-Y dye borne in a carrier of ethylene glycol to measure O_3 concentration at high frequencies (Ray et al., 1986; Katul et al., 1996a). However, the chemiluminescent reaction of O_3 with eosine-Y decreases appreciably the signal-to-noise ratio (SNR) of such gas analyzers thus prohibiting effective use of these measurements to investigating higher-order turbulence moments (Lenschow, 1982) or organized eddy motion responsible for the exchange of O_3 between the forest and the atmosphere. A sample run of longitudinal (u') and vertical (w') velocities, temperature, and ozone concentrations are shown in Fig. 1. It is evident

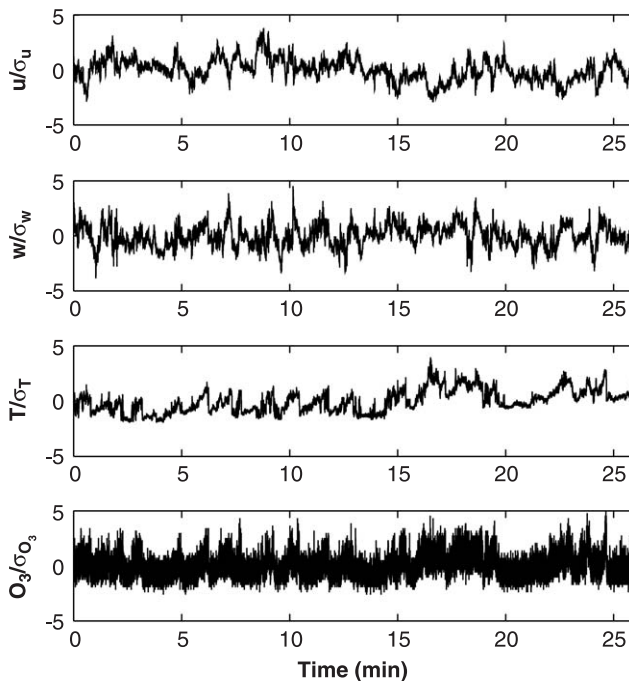


Fig. 1. Time series of simultaneously measured turbulent velocity components, air temperature, and ozone concentration. For comparison purposes, all the time series measurements are normalized to zero-mean and unit variance.

that the velocities and air temperature are not contaminated by the type of noise present in the O_3 measurements. The model that will separate the noise from the “true” turbulence signal for O_3 is considered next.

2.2. The Bayesian model

Suppose the observed data \mathbf{y} (e.g., ozone concentrations) represent the sum of an unknown signal \mathbf{s} and random noise $\boldsymbol{\epsilon}$. Coordinatewise,

$$\mathbf{y}_i = \mathbf{s}_i + \boldsymbol{\epsilon}'_i, \quad i = 1, \dots, n. \quad (1)$$

In the wavelet domain (after applying a nondecimated wavelet transformation W to the observed data), expression (1) becomes $d_{jk} = \theta_{jk} + \varepsilon_{jk}$, where d_{jk} , θ_{jk} , and ε_{jk} are the j, k th coordinates in the traditional nondecimated scale/shift wavelet-enumeration of vectors $W\mathbf{y}$, $W\mathbf{s}$ and $W\boldsymbol{\epsilon}'$, respectively. For completeness, a brief overview of nondecimated wavelet transformations is provided in Appendix B. Our assumption is that the coefficients d_{jk} can be considered independent, at least for high resolution levels. This assumption is reasonable due to the so-called *decorrelation property* of wavelets (Flandrin, 1999). The decorrelation property is sensitive to the choice of the analyzing wavelet with high decorrelation commonly achieved using the Haar basis. Its inherited locality and decorrelation properties are the primary reasons for our choice of the Haar basis in such applications. In the exposition that follows, we omit the double index jk and work with a “typical” wavelet coefficient, d .

It is now standard practice in model-induced wavelet shrinkage to specify a location model on the wavelet coefficients, elicit the prior on their locations (the signal part in wavelet coefficients), exhibit the Bayes estimator for the locations and, if the resulting Bayes rules are shrinkage estimators, apply the inverse wavelet transformation to the estimators. We assume, as commonly done, that each coefficient d in the wavelet domain is affected by normal errors, and thus the conditional distribution of d given θ and σ^2 , $[d|\theta, \sigma^2]$, is $\mathcal{N}(\theta, \sigma^2)$. In BAMS, the prior distributions on σ^2 and θ are chosen to be, respectively, an exponential one, $\mathcal{E}(\mu)$, and a mixture of a point mass at zero and a double exponential distribution, $\mathcal{D}\mathcal{E}(0, \tau)$.

The Bayes rule is

$$\delta^*(d) = \frac{(1 - \varepsilon)m(d)\delta(d)}{(1 - \varepsilon)m(d) + \varepsilon\mathcal{D}\mathcal{E}(0, 1/\sqrt{2\mu})}, \quad (2)$$

where

$$m(d) = \frac{\tau e^{-|d|/\tau} - (1/\sqrt{2\mu})e^{-\sqrt{2\mu}|d|}}{2\tau^2 - 1/\mu}.$$

This rule is close to a thresholding rule because it heavily shrinks small-in-magnitude arguments with minor influence on the larger arguments. The BAMS method is implemented in the MATLAB toolbox of Antoniadis, Bigot, and Sapatinas (Antoniadis et al., 2001) available at <http://www-lmc.imag.fr/SMS/software/GaussianWaveDen/>.

2.3. Tuning the model parameters

One of the main issues in any Bayesian analysis is the elicitation of the hyperparameters specifying the statistical model. Often the hyperparameters may have their own priors, leading to hierarchical models.

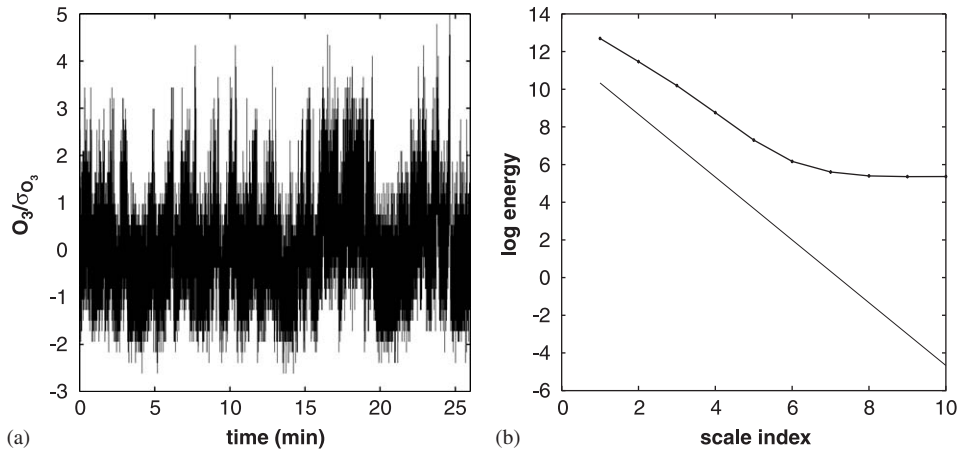


Fig. 2. Left: The original (normalized) ozone concentration time series sampled at 21 Hz. Right: The Haar wavelet-spectra of the time series demonstrating that the observations contain noise (flattening of spectral line) at the high resolution levels (or for a large scale index). For reference, the **K41** power-law is also shown.

The described model depends on three hyperparameters that have to be a priori specified. Purely subjective elicitation of priors is difficult since, in general, users may lack intuition and interpretation of wavelet-domain priors. Subjective priors can be easily elicited only when the prior information concerns smoothness or self-similarity. A variety of default solutions are available, but default choices do not seem to be very suitable in function estimation, since observations can vary tremendously and some degree of informativeness and/or data dependence should be exploited.

Vidakovic and Ruggeri (2001) proposed an empirical moment matching specification of parameters which worked well if the signal is smooth. In this paper, the parameter specification will reflect the fact that signals are self-similar with theoretically established Hurst exponent $H = \frac{1}{3}$.

1. μ is the reciprocal of the mean for the prior on σ^2 , or, equivalently, the square root of the precision for σ^2 . We first estimate σ by a robust Tukey's $\text{pseudos} = (Q_3 - Q_1)/C$, where Q_1 and Q_3 are the first and the third quartile of the finest level of details in the decomposition and $1.3 \leq C \leq 1.5$. We propose $1/\text{pseudos}$ as a default value for μ ; according to the Law of Large Numbers, this ratio should be close to the "true" μ .
2. ε is the weight of the point mass at zero in the prior on θ and should depend on level j . If the signal is smooth ε should be close to 1 at the finest level of detail and near 0 at coarse levels. In our case the signal is not smooth and a decay in ε is unreasonable. Hence, we fixed $\varepsilon = 0.5$ in all levels. With a constant ε , control of prior variance decay becomes easier though we emphasize that the value of $\varepsilon = 0.5$ is not unique.
3. The parameter τ is the scale of the "spread part" in the prior (4), see Appendix A. In the case of a double exponential prior, the variance of the signal part is $2\tau^2$. Because of assumed independence between the error and the signal parts, we have $\sigma_d^2 = 2(1 - \varepsilon)^2\tau^2 + 1/\mu$, where σ_d^2 is the variance of an observation d . According to **K41** exact power laws, the average energies of the signal in the wavelet domain decay in a log-linear fashion when increasing the resolution of the levels (or the level index). This provides a calibration method for eliciting prior variances on the signal coefficients: they decay proportionally to $2^{(-5/3)}$.

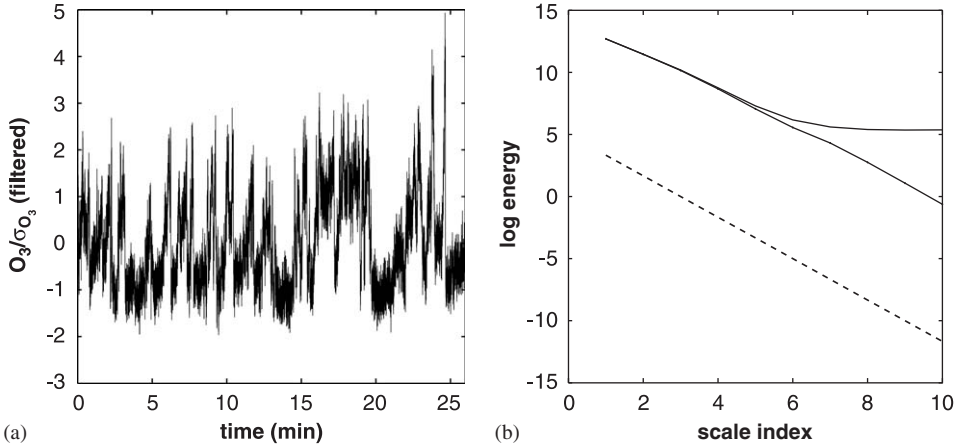


Fig. 3. Left: The (normalized) filtered times series (s_i) derived from the infected time series (y_i) of Fig. 2. Right: The Haar wavelet power spectrum of the filtered time series s_i . For reference, we also repeat the Haar wavelet spectrum of y_i from Fig. 2. The dotted line is the theoretical **K41** power-law.

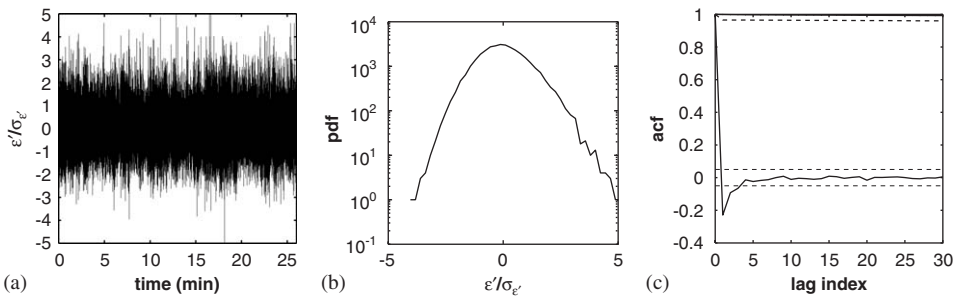


Fig. 4. Left: Time series of the (normalized) residuals ($\epsilon'_i = y_i - s_i$). Center: The probability density function (pdf) of ϵ'_i suggesting marginal normality (near-parabola in the log-scale). Right: The autocorrelation function (acf) of ϵ'_i (solid), s_i (dotted), and y_i (dot-solid) as a function of the lag index. For ϵ'_i , the 95% confidence levels demonstrate reasonable whiteness. Note that top dot-solid line for y_i hardly decayed after 30 lags (≈ 1.4 s).

Unlike the thresholding rules that set small wavelet coefficients to 0, the rule (2) splits the coefficients as $d = \delta^*(d) + (d - \delta^*(d)) = \hat{\theta} + \hat{\epsilon}$. The $\hat{\theta}$ -part corresponds to turbulence signal and exhibits energy spectra decaying with a slope of $-\frac{5}{3}$ ($H = \frac{1}{3}$) due to pre-described scaling. On the other hand, the noise part coefficients, $\hat{\epsilon}$, exhibit “flat” spectra, as expected.

The process of filtering is illustrated in Figs. 2–4. Fig. 2(a) shows the original O_3 concentration time series measurements. Not only is the noise present but also the measurements appear quantized (rounded to a small discrete set of values) by the instrument. Fig. 2(b) shows the Haar wavelet power spectra of the measurements shown in panel (a). Note the flattening of the spectra for fine scales in which the energy of noise exceeds the energy of the signal.

Fig. 3 shows the filtered (i.e., turbulent) signal spectrally and in the time domain. It is evident that the filtered signal recovers well **K41** scaling. Fig. 4 represents the residuals (i.e., noise) along with their histogram (on a log scale), and their autocorrelation function. What remains to

be investigated is the faithfulness of the filtering scheme to recovering the theoretical statistical properties of high Reynolds number flows.

3. Battery of tests

The Bayes rule $\hat{\theta}(d)$ divides the wavelet coefficient in two components, $d = \hat{\theta} + (d - \hat{\theta})$. The inverse wavelet image of all $\hat{\theta}$ correspond to filtered time series, while the inverse image of $\hat{e} = d - \hat{\theta}$ corresponds to the noise component, vector $\tilde{e} = (e_1, \dots, e_n)$ in the time domain.

The filtering algorithm must be capable of removing the noise levelwise without distorting any interaction between ozone and velocity fluctuations at multiple scales. Specifically, we tested whether (i) the Haar wavelet co-spectra between measured vertical velocity and filtered ozone concentration follows a $-\frac{7}{3}$ **K41** power law, and (ii) whether the mixed structure function defined by

$$D_{w'O_3O_3}(\tau) = \langle \Delta_{O_3}^2(\tau) \Delta_{w'}(\tau) \rangle,$$

where angular brackets represent averaging, $\Delta_G(\tau) = G(t + \tau) - G(t)$ and G is any turbulent flow variable, follows a τ^1 power-law as in Katul et al. (1997a) for locally homogeneous and isotropic turbulence. We emphasize that the two proposed battery of tests are entirely independent of the filtering scheme since they consider interactions between filtered O_3 and the velocity measurements shown in Fig. 1 but not used in the filtering scheme. Based on **K41**, the battery of tests above are applicable to any scalar fluctuations in the inertial subrange. In this experiment, air temperature fluctuations T were also measured with high precision (see Fig. 1) and hence can be used as an additional line of testing on the applicability of the battery of tests. That is, the T time series can be used to assess how valid are the local homogeneity and isotropy approximations of **K41** theory for these experimental conditions.

In Fig. 5, the co-spectra between w' and the ozone time series (filtered and raw) along with **K41** power-laws and the measured co-spectra between w' and T , and w' and u' are shown for

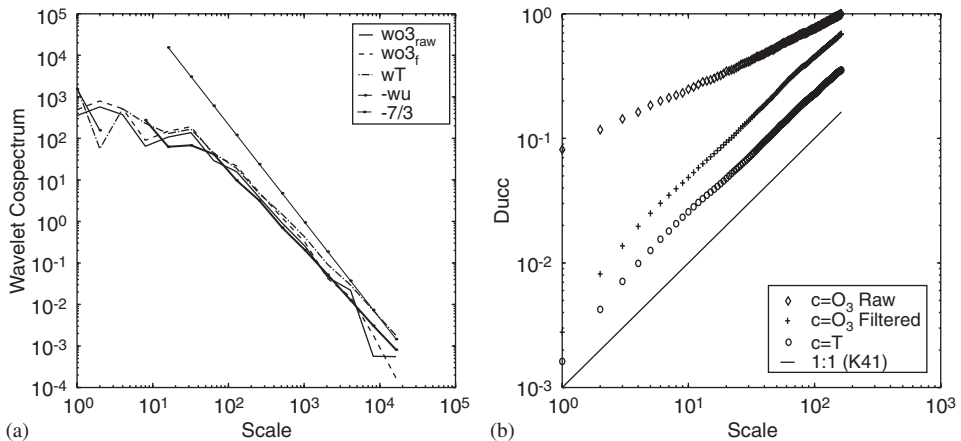


Fig. 5. Left: Computed Haar wavelet co-spectra for filtered and raw O_3 time series with w' . For reference the co-spectra between w' and air temperature T and w' and u' are shown along with **K41** power-laws. Right: Computed mixed structure functions ($D_{w'CC}$) for C representing filtered and raw O_3 time series with u' . For reference, the mixed structure function between T and u' is also shown along with τ^1 from **K41**.

reference. It is clear that the filtering scheme did not distort the co-spectral properties of w' , O_3 as evidenced from their spectral similarity to w' , T . However, Fig. 5 clearly demonstrates that the mixed structure function $D_{u'O_3O_3}(\tau)$ power-laws for the filtered O_3 time series is much closer to the measured $D_{u'TT}(\tau)$ than the unfiltered O_3 . Hence, the filtering scheme clearly recovered the theoretical mixed velocity-scalar moments in the inertial subrange associated with high Reynolds number flows. We note that $D_{u'O_3O_3}$ is a more sensitive test because the $\Delta_{O_3}^2$ contribution to $D_{u'O_3O_3}$ is more influenced by instrument noise when compared to the co-spectrum between w' and O_3 .

In short, interactions between the filtered O_3 time series and turbulent velocity (u' , w') are more consistent with theoretical predictions from turbulence theories (e.g. **K41**) than the unfiltered ozone time series.

Although marginally normal, the residuals e_k are not exactly “white”. We found that in separated noise there are significant 2- to 3-lag autocorrelations. In the run we explored the empirical model for the noise is found to be

$$e_k - 0.2971 * e_{k-1} - 0.2056 * e_{k-2} - 0.1605 * e_{k-3} = Z_n,$$

where Z_n is a white noise time series.

This finding is in agreement with the physical properties of the chemiluminescent gas analyzer, in which some residual reactants from previous sampling times influence the present ozone concentration measurement.

4. Conclusions

The novelty of the filtering scheme proposed in this paper is twofold. First we have chosen nondecimated wavelet transformations in order to address the self-similarity locally. Although the power spectra utilized in the BAMS method is calculated globally, the number of local slopes used to calculate average level energies does not decrease when the levels shift from fine to coarse. This ensures more stable estimators of power spectra, especially for the coarse detail levels.

The second novelty of the method is in its application. The BAMS method, which was earlier tested in the case of smooth signals, is now extended to signals' exhibiting fractality. Such application was possible after establishing a connection between the geophysical phenomenon (power-laws) and the prior elicitation in the model driving the BAMS method (variance decay).

Vidakovic et al. (2000) considered a problem of denoising the fractional Brownian motion $fBm(1/3)$ as a simplified model for a turbulent signal. They explored three techniques: Fourier amplitude shrinkage (FAS) that splits Fourier coefficients obtained by FFT, wavelet amplitude shrinkage (WAS) that applies linear shrinkage on magnitudes of wavelet coefficients, and Bayesian energy fraction estimation (BEFE) that uses normal model-normal prior structure in performing the filtering. Although all three methods are effective and comparable, BAMS method differs from the above techniques in two ways: (i) the models (marginal likelihood and prior) in BAMS are more realistic, that is, better fit the real observed data, and (ii) BAMS uses nondecimated wavelets (although critically sampled orthogonal wavelets can be used as well).

The broad outcome of this application is a filtering methodology ideally suited for separating high frequency O_3 time series measurements from an autoregressive noise. Such measurements can be used to infer higher-order turbulence statistics for O_3 and organized motion responsible for O_3 exchange between the forest and the atmosphere. Schemes such as surface renewal (Katul et al., 1996b) can also take advantage of such filtered time series to predict fluxes.

Appendix A. Bayes rule

The model $[d|\theta, \sigma^2] \sim \mathcal{N}(\theta, \sigma^2)$ is completed by eliciting priors on θ and σ^2 . The choice of an exponential prior for σ^2 is justified since it is an entropy maximizer in the class of all distributions supported on $(0, \infty)$ with a fixed first moment. The choice of a double exponential component in the mixture point-mass prior on θ is based on inspecting the empirical realizations of coefficients of pure signals, and decision theoretical recommendations by Ruggeri and Vidakovic (1999), whereas the point-mass-at-zero component ensures the enhanced and possibly adaptive shrinkage by the resulting Bayes rule, as shown in Vidakovic and Ruggeri (1999).

Besides, adequate changes in ε , the weight of the point mass, and the parameter of the double exponential distribution make it possible to adapt the shrinkage rules levelwise.

Starting with $[d|\theta, \sigma^2] \sim \mathcal{N}(\theta, \sigma^2)$ and the prior $\sigma^2 \sim \mathcal{E}(\mu)$, $\mu > 0$, with density $f(\sigma^2|\mu) = \mu e^{-\mu\sigma^2}$, we obtain the marginal likelihood

$$d|\theta \sim \mathcal{DE}\left(\theta, \frac{1}{\sqrt{2\mu}}\right) \quad \text{with density } f(d|\theta) = \frac{1}{2} \sqrt{2\mu} e^{-\sqrt{2\mu}|d-\theta|}.$$

If the prior on θ is

$$[\theta] \sim \mathcal{DE}(0, \tau),$$

then the predictive distribution $m(d)$ is

$$[d] \sim m(d) = \frac{\tau e^{-|d|/\tau} - (1/\sqrt{2\mu})e^{-\sqrt{2\mu}|d|}}{2\tau^2 - 1/\mu},$$

and the corresponding Bayes rule with respect to the squared error loss is

$$\delta(d) = \frac{\tau(\tau^2 - 1/(2\mu))de^{-|d|/\tau} + \tau^2(e^{-|d|\sqrt{2\mu}} - e^{-|d|/\tau})/\mu}{(\tau^2 - 1/(2\mu))(\tau e^{-|d|/\tau} - (1/\sqrt{2\mu})e^{-|d|\sqrt{2\mu}})}. \tag{3}$$

Rule (3) is a shrinkage one, but it is close to a linear shrinkage rule, known to be underperforming in wavelet-based methods.

Rules with a more desirable shape result from the ε -contaminated priors, with a point mass at zero. When

$$[\theta|\varepsilon] \sim \varepsilon\delta_0 + (1 - \varepsilon)\mathcal{DE}(0, \tau), \tag{4}$$

the marginal is

$$d \sim m^*(d) = \varepsilon\mathcal{DE}\left(0, \frac{1}{\sqrt{2\mu}}\right) + (1 - \varepsilon)m(d),$$

and the Bayes rule is

$$\delta^*(d) = \frac{(1 - \varepsilon)m(d)\delta(d)}{(1 - \varepsilon)m(d) + \varepsilon\mathcal{DE}(0, 1/\sqrt{2\mu})}.$$

This rule is depicted in Fig. 6 for some specific values of hyperparameters.

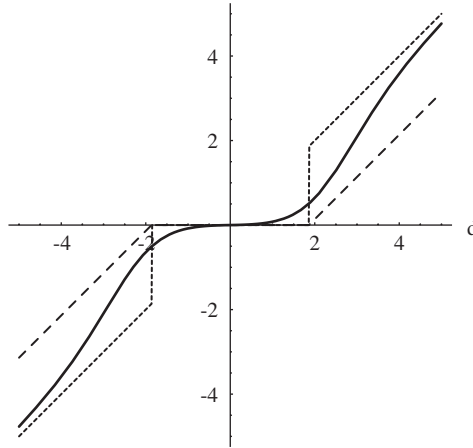


Fig. 6. Bayes rule $\delta(d)$ for $\varepsilon = 0.9$, $\tau = 2$, and $\mu = \frac{1}{2}$.

Appendix B. Non-decimated wavelet transformations

For quadrature mirror wavelet filters \tilde{h} and \tilde{g} , we define recursively up-sampled filters $\tilde{h}^{[r]}$ and $\tilde{g}^{[r]}$

$$\begin{aligned} \tilde{h}^{[0]} &= \tilde{h}, & \tilde{g}^{[0]} &= \tilde{g}, \\ \tilde{h}^{[r]} &= [\uparrow 2]\tilde{h}^{[r-1]}, & \tilde{g}^{[r]} &= [\uparrow 2]\tilde{g}^{[r-1]}. \end{aligned}$$

In practice, the dilated filter $\tilde{h}^{[r]}$ is obtained by inserting zeroes between the taps in $\tilde{h}^{[r-1]}$. Let $\mathbf{H}^{[r]}$ and $\mathbf{G}^{[r]}$ be convolution operators with filters $\tilde{h}^{[r]}$ and $\tilde{g}^{[r]}$, respectively. A non-decimated wavelet transformation, NDWT, is defined as a sequential application of operators (convolutions) $\mathbf{H}^{[j]}$ and $\mathbf{G}^{[j]}$ on a given time series.

Definition. Let $\tilde{a}^{(J)} = \tilde{c}^{(J)}$ and

$$\begin{aligned} \tilde{a}^{(j-1)} &= \mathbf{H}^{[J-j]}\tilde{a}^{(j)}, \\ \tilde{b}^{(j-1)} &= \mathbf{G}^{[J-j]}\tilde{a}^{(j)}. \end{aligned}$$

The non-decimated wavelet transformation of $\tilde{c}^{(J)}$ is $\tilde{b}^{(J-1)}, \tilde{b}^{(J-2)}, \dots, \tilde{b}^{(J-j)}, \tilde{a}^{(J-j)}$, for some $j \in \{1, 2, \dots, J\}$ the depth of the transformation.

If the length of an input vector $\tilde{c}^{(J)}$ is 2^J , then for any $0 \leq m < J$, $\tilde{a}^{(m)}$ and $\tilde{b}^{(m)}$ are of the same length. Let $\phi_j(x) = \phi_{j,0}(x)$ and $\psi_j(x) = \psi_{j,0}(s)$. If the measurement sequence $\tilde{c}^{(J)}$ is associated

with the function $f(x) = \sum_k c_k^{(j)} \phi_j(x - 2^{-j}k)$ then the k th coordinate of $\tilde{b}^{(j)}$ is equal to

$$b_{jk} = \int \psi_j(x - 2^{-j}k) f(x) dx.$$

Thus, the coefficient b_{jk} provides information at scale 2^{J-j} and location k . One can think of a nondecimated wavelet transformation as sampled continuous wavelet transformation $\langle f(x), (1/\sqrt{a})\psi((x-b)/a) \rangle$ for $a = 2^{-j}$, and $b = k$.

References

- Antoniadis, A., Bigot, J., Sapatinas, T., 2001. Wavelet estimators in nonparametric regression: a comparative simulation study. *J. Statist. Soft.* 6, 1–83 <<http://www-lmc.imag.fr/SMS/software/GaussianWaveDen/>>.
- Berliner, M., Wikle, C., Milliff, R., 1999. Multiresolution wavelet analyses in hierarchical Bayesian turbulence models. In: Müller, Vidakovic (Eds.), *Bayesian Inference in Wavelet Based Models*, Lecture Notes in Statistics, vol. 141. Springer, Berlin, pp. 341–349.
- Farge, M., 1992. Wavelet transforms and their applications to turbulence. *Annual Rev. Fluid Mech.* 24, 395–457.
- Farge, M., Goirand, E., Meyer, Y., Pascal, F., Wickerhauser, M.V., 1992. Improved predictability of two-dimensional turbulent flows using wavelet packet compression. *Fluid Dynamics Research* 10, 229–250.
- Flandrin, P., 1999. *Time-Frequency/Time-Scale Analysis*. Academic Press, San Diego, CA, 386pp.
- Hudgins, L., Friche, C., Mayer, M., 1993. Wavelet transforms and atmospheric turbulence. *Phys. Rev. Lett.* 71, 3279–3282.
- Katul, G.G., Vidakovic, B., 1998. Identification of low-dimensional energy containing/flux transporting eddy motion in the atmospheric surface layer using wavelet thresholding methods. *J. Atmospheric Sci.* 54, 91–103.
- Katul, G.G., Finkelstein, P.L., Clarke, J.F., Ellstad, T.G., 1996a. An investigation of the conditional sampling method used to estimate fluxes of active, reactive, and passive scalars. *J. Appl. Meteorology* 35, 1835–1845.
- Katul, G.G., Hsieh, C.I., Ellsworth, D., Oren, R., Phillips, N., 1996b. Latent and sensible heat fluxes from a uniform pine forest using surface renewal and flux variance methods. *Boundary Layer Meteorology* 80, 249–282.
- Katul, G.G., Hsieh, C.I., Sigmon, J., 1997a. Energy-inertial scale interaction for temperature and velocity in the unstable surface layer. *Boundary Layer Meteorology* 82, 49–80.
- Katul, G.G., Hsieh, C.I., Kuhn, G., Ellsworth, D., Nie, D., 1997b. The turbulent eddy motion at the forest-atmosphere interface. *J. Geophys. Res.* 102, 13409–13421.
- Kolmogorov, A.N., 1941. The local structure of turbulence in incompressible viscous fluid for very large Reynolds numbers. *Dokl. Akad. Nauk. SSSR* 30, 301–305.
- Kumar, P., Foufoula-Georgiou, E., 1993. A multicomponent decomposition of spatial rainfall fields: 2. Self-similarity in fluctuations. *Water Resour. Res.* 29, 2533–2544.
- Kumar, P., Foufoula-Georgiou, E., 1994. Wavelet analysis in geophysics: an introduction. In: Foufoula-Georgiou, Kumar (Eds.), *Wavelets in Geophysics*. Academic Press, New York, pp. 1–43.
- Lenschow, D.H., 1982. Reactive trace species in the boundary layer from a micrometeorological perspective. *J. Meteorological Soc. Japan.* 60, 472–480.
- Ray, J., Stedman, D., Wendel, G., 1986. Fast chemiluminescent method for measurement of ambient ozone. *Anal. Chem.* 58, 598–600.
- Ruggeri, F., Vidakovic, B., 1999. Bayesian decision theoretic approach to the choice of thresholding parameter. *Statistica Sinica* 9, 183–197.
- Shi, B., Vidakovic, B., Katul, G., Albertson, J., 2005. Assessing the effects of atmospheric stability on the fine structure of surface layer turbulence using local and global multiscale approaches. *Phys. Fluids* 17, 1–12 (0545104).
- Vattay, G., Harnos, A., 1994. Scaling behavior in daily air humidity fluctuations. *Phys. Rev. Lett.* 73, 768.
- Vergassola, M., Frisch, U., 1991. Wavelet transforms of self-similar processes. *Physica D* 54, 58–64.
- Vidakovic, B., Ruggeri, F., 1999. Expansion estimation by Bayes rules. *J. Statist. Plann. Inference* 79, 223–235.
- Vidakovic, B., Ruggeri, F., 2001. BAMS method: theory and simulations. *Sankhya B* 63, 234–249.
- Vidakovic, B., Katul, G., Albertson, J., 2000. Multiscale denoising of self-similar processes. *J. Geophys. Res. Atmos.* 105 (D22), 27049–27058.
- Wikle, C., Berliner, M., Cressie, N., 1998. Hierarchical Bayesian space-time models. *J. Environmental and Ecological Statistics* 5, 117–154.
- Zubair, L., Sreenivasan, K., Wickerhauser, M., 1991. Compression of turbulence data and images using wavelet packets. In: Gadsby, T., Sirkar, S., Speziale, C. (Eds.), *Studies in Turbulence*. Springer, Berlin, pp. 489–513.